The impact of human-induced climate change on future tornado intensity as revealed through multi-scale modeling

Matthew J. Woods[1]†, Robert J. Trapp[2], and Holly M. Mallinson[3]

[1]Department of Atmospheric Sciences, University of Illinois.

[2]Department of Atmospheric Sciences, University of Illinois.

[3]Department of Atmospheric Sciences, University of Illinois.

Corresponding author: Robert J. Trapp (jtrapp@illinois.edu)

†Current affiliation: National Weather Service, Las Vegas, NV.

Supplementary Material

Tornado intensification results from vortex stretching, which is dynamically equivalent to conservation of circulation Γ. For an axisymmetric vortex with a uniform core of vorticity on a horizontal plane, circulation is

$$\Gamma = \zeta \pi R^2 \qquad (1)$$

where R is vortex-core radius, and ζ is the vertical component of the vorticity vector. For such an axisymmetric vortex, we can also write:

$$\Gamma = 2\pi R V \qquad (2)$$

where V is the tangential speed of the vortex at radius R. Using (1) and (2), the vertical vorticity of the vortex can thus be expressed as:

$$\zeta = 2V/R \qquad (3)$$

Note here that we can obtain Eq. (3) directly by using the definition of vertical vorticity in polar coordinates,

$$\zeta = \frac{1}{r}\frac{\partial (r u_\theta)}{\partial r} - \frac{1}{r}\frac{\partial u_r}{\partial \theta} \qquad (4)$$

and then substituting $u_r = 0$, $u_\theta = V\,r/R$, where u_θ and u_r are the tangential and radial velocity components, respectively.

If we evaluate Eq. (3) with $R = 100$ m, then for a weak (i.e., EF0), strong (i.e., EF2), and violent (i.e., EF4) tornado, with $V = 30$ m s^{-1}, $V = 50$ m s^{-1}, and $V = 75$ m s^{-1}, respectively, we find that $\zeta = 0.6$ s^{-1}, $\zeta = 1.0$ s^{-1}, and $\zeta = 1.5$ s^{-1}. Thus, in an idealized vortex with a fixed core radius, vortex intensity is quantified well by vertical vorticity.

Unsurprisingly, these estimates based on an idealized vortex model are of the same order of magnitude as the 10^0 s^{-1} estimate based on typical scale analysis (e.g., Trapp 2013). In real tornadoes with asymmetric, non-uniform cores observed using discrete data, the magnitude of the calculated vertical vorticity depends on the resolution of the data used in the calculations. As would be the case for extrema of any field represented in discrete data, it is logical to expect that the "true" value of ζ will be reduced in coarsened data. This explains why, for example, Coffer et al. (2017) and Gray and Frame (2021) used vertical vorticity thresholds of 0.3 s^{-1} and 0.15 s^{-1}, respectively, for "tornado-like vortex" (TLV) identification on horizontal grids with 125 m and 250 m spacings. A key point here is that the thresholds in these and many other studies are obtained heuristically.

We can, however, demonstrate support of these heuristic estimates by calculating the vertical vorticity of an idealized tornado on a Cartesian grid with different spacings in x and y, i.e., Δx and Δy. Let:

$$u_\theta = \begin{cases} \frac{Vr}{R}, r \le R \\ \frac{VR}{r}, r > R \end{cases} \quad (5)$$

which models a Rankine vortex with a uniform core of vorticity surrounded by irrotational flow; despite its idealization, Eq. (5) also approximates the rotational flow in real tornadoes to varying degrees (e.g., Wurman & Gill, 2000). For consistency with the discussion above, we initially let $R = 100$ m and $V = 50$ m s^{-1}, and thus per Eq. (3), $\zeta = 1.0$ s^{-1} within the core. The arbitrary domain for our calculations is $0 \le x, y \le 5000$ m, and the vortex is centered at $x_o, y_o = 2500$ m. Upon implementing Eq. (5) using $r = \sqrt{(x - x_o)^2 + (y - y_o)^2}$, the resulting velocity field is transformed into Cartesian coordinates, and then $\zeta (= \partial v/\partial x - \partial u/\partial y)$ is determined using centered finite differencing.

On a grid with $\Delta x = 10$ m $= \Delta y$, which resolves well a 200-m diameter vortex, the calculated maximum vertical vorticity is $\hat{\zeta} = 1.0$ s^{-1}, implying that the tornadic vortex intensity is fully represented (Fig. A). If we coarsen the grid to $\Delta x = 250$ m $= \Delta y$, we no longer resolve the vortex, yet Fig. B still reveals a vortex signature, with $\hat{\zeta} = 0.16$ s^{-1}; notice that this vertical vorticity value is nearly the same as Gray and Frame (2021)'s threshold of 0.15 s^{-1} used for TLV identification in model simulations with 250 m grid spacing. If we further coarsen the grid to $\Delta x = 1000$ m $= \Delta y$, which is the grid spacing used in regional model simulations of this study, a size-exaggerated signature of the vortex continues to exist, with $\hat{\zeta} = 0.008$ s^{-1} (Fig. C). Finally, if we increase the tangential windspeed to $V = 75$ m s^{-1}, we find a size-exaggerated signature of the vortex with a larger calculated vertical vorticity, $\hat{\zeta} = 0.012$ s^{-1} (Fig. D). In other words, the increased intensity of a tornadic vortex is represented on a coarse grid as an increase in maximum vertical vorticity, even though the tornado itself is under-resolved.

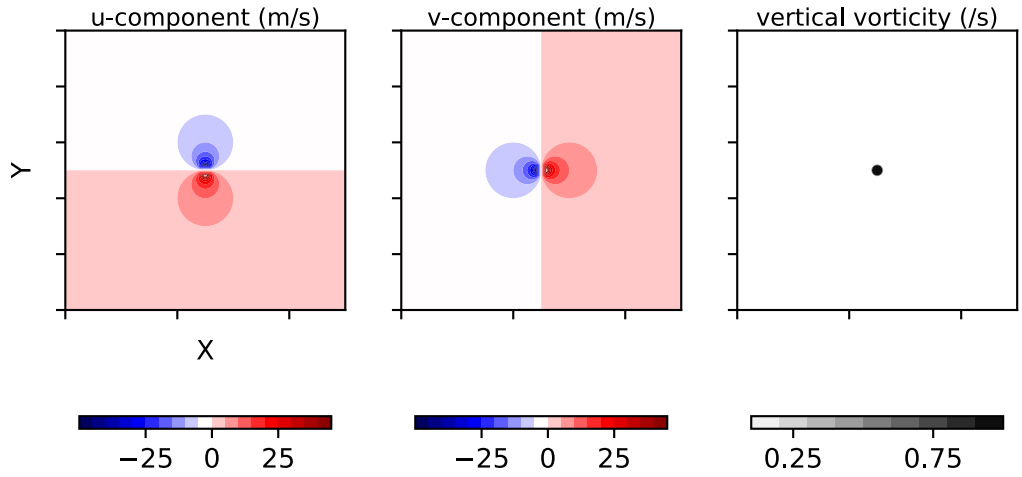

Fig. A. Cartesian component velocities and vertical vorticity for the case $\Delta x = 10$ m, $V = 50$ m s^{-1}, in which $\hat{\zeta} = 1.0$ s^{-1}.

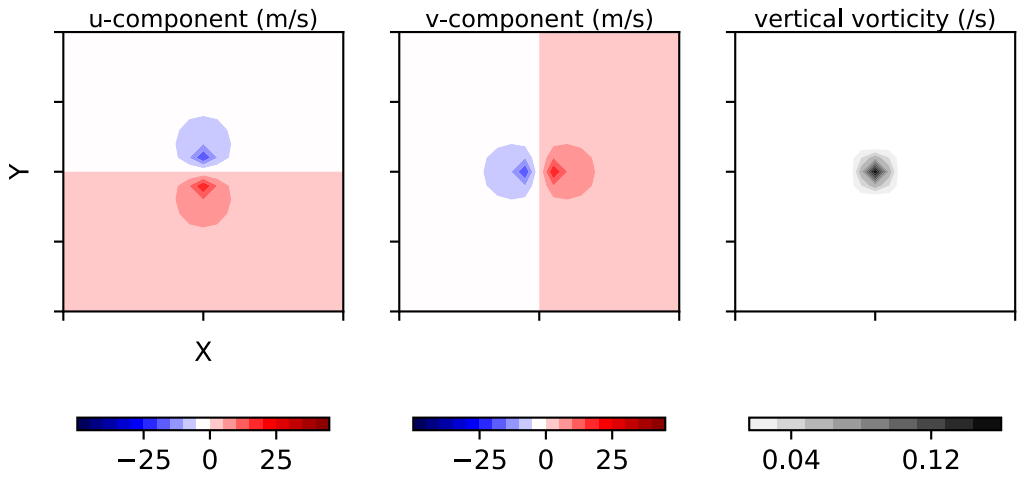

Fig. B. As in Fig. A, except for Cartesian component velocities and vertical vorticity for the case case $\Delta x = 250$ m, $V = 50$ m s^{-1}, in which $\hat{\zeta} = 0.16$ s^{-1}.

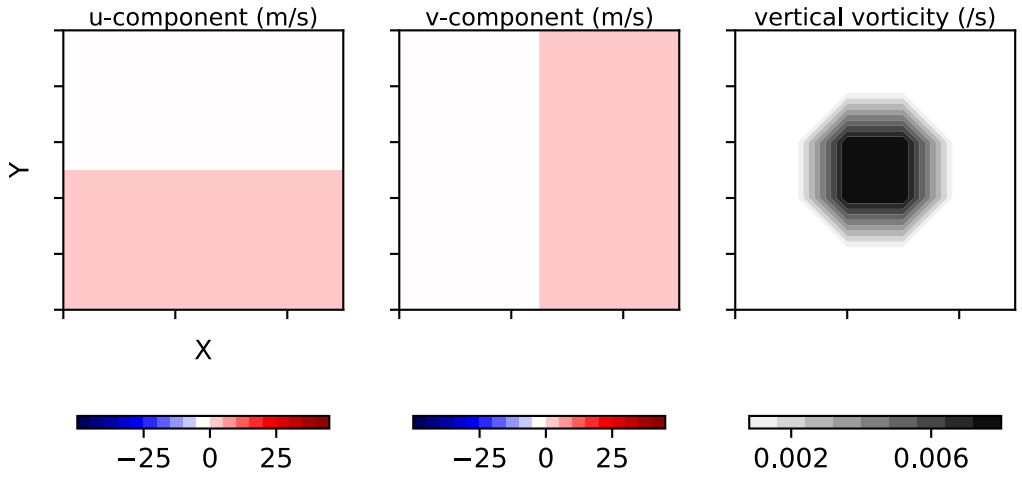

Fig. C. As in Fig. A, except for Cartesian component velocities and vertical vorticity for the case case $\Delta x = 1000$ m, $V = 50$ m s^{-1}, in which $\hat{\zeta} = 0.008$ s^{-1}.

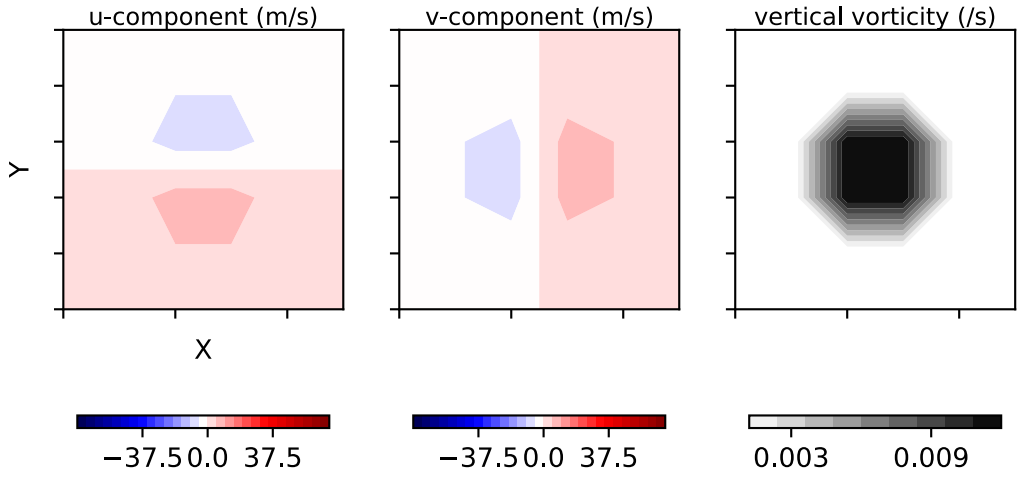

Fig. D. As in Fig. A, except for Cartesian component velocities and vertical vorticity for the case $\Delta x = 1000$ m, $V = 75$ m s^{-1}, in which $\hat{\zeta} = 0.012$ s^{-1}.

The essence of this simple exercise is also revealed in the observational results of Toth et al. (2013; see their section 3), which show high linear correlation between quantifications of tornado intensity (differential velocity) obtained near the surface with high-resolution mobile radar and quantifications of the corresponding tornadic-vortex/mesocyclone intensity determined using the coarser-resolution measurements of the nearest WSR-88D. To be clear, the vortex sampled by a WSR-88D represents some combination of the tornado and its ambient circulation. The essence of the exercise is also reflected in the ongoing efforts to estimate tornado intensity–as manifest by degree of damage, and represented through an EF rating–using radar-quantified characteristics of the mesocyclone or tornadic vortex (e.g., Smith et al. 2020).

Thus, as justified by observational data as well as by analyses of a discretized vortex model, we use magnitudes of vertical vorticity as potential tornado proxies in our regional model simulations with 1-km grid spacings. The vertical vorticity is evaluated at a height of 80 m, which is approximately the height of the first model level above the lower model boundary. Consistent with the vortex-model analysis results, a vertical vorticity value locally exceeding 0.0075 s^{-1}, which is the 99th percentile of gridpoint values in the CTRL simulation, serves as a tornado proxy occurrence. A vertical vorticity value exceeding 0.0125 s^{-1}, which is the 99.9th percentile, serves as a significant tornado proxy occurrence. Coexistence of local updraft velocities exceeding 5 m s^{-1} is required.

References

Coffer, B. E., Parker, M. D., Dahl, J. M. L., Wicker, L. J., & Clark, A. J. (2017). Volatility of tornadogenesis: An ensemble of simulated nontornadic and tornadic supercells in VORTEX2 environments. Monthly Weather Review, 145, 4605-4625, https://doi.org/10.1175/MWR-D-17-0152.1.

Gray, K., & Frame, J. (2021). The impact of midlevel shear orientation on the longevity of and downdraft location and tornado-like vortex formation within simulated supercells. *Monthly Weather Review*, 149, 3739-3759, https://doi.org/10.1175/MWR-D-21-0085.1

Smith, B. T., Thompson, R. L., Speheger, D. A., Dean, A. R., Karstens, C. D., & Anderson-Frey, A. K. (2020). WSR-88D Tornado Intensity Estimates. Part II: Real-Time Applications to Tornado Warning Time Scales. *Weather and Forecasting*, 35, 2493–2506, https://doi.org/10.1175/WAF-D-20-0011.1.

Trapp, R. J. (2013). *Mesoscale-Convective Processes in the Atmosphere*. Cambridge University Press.

Wurman, J., & Gill, S. (2000). Finescale Radar Observations of the Dimmitt, Texas (2 June 1995), Tornado. *Monthly Weather Review*, 128, 2135–2164, https://doi.org/10.1175/1520-0493(2000)128<2135:FROOTD>2.0.CO;2

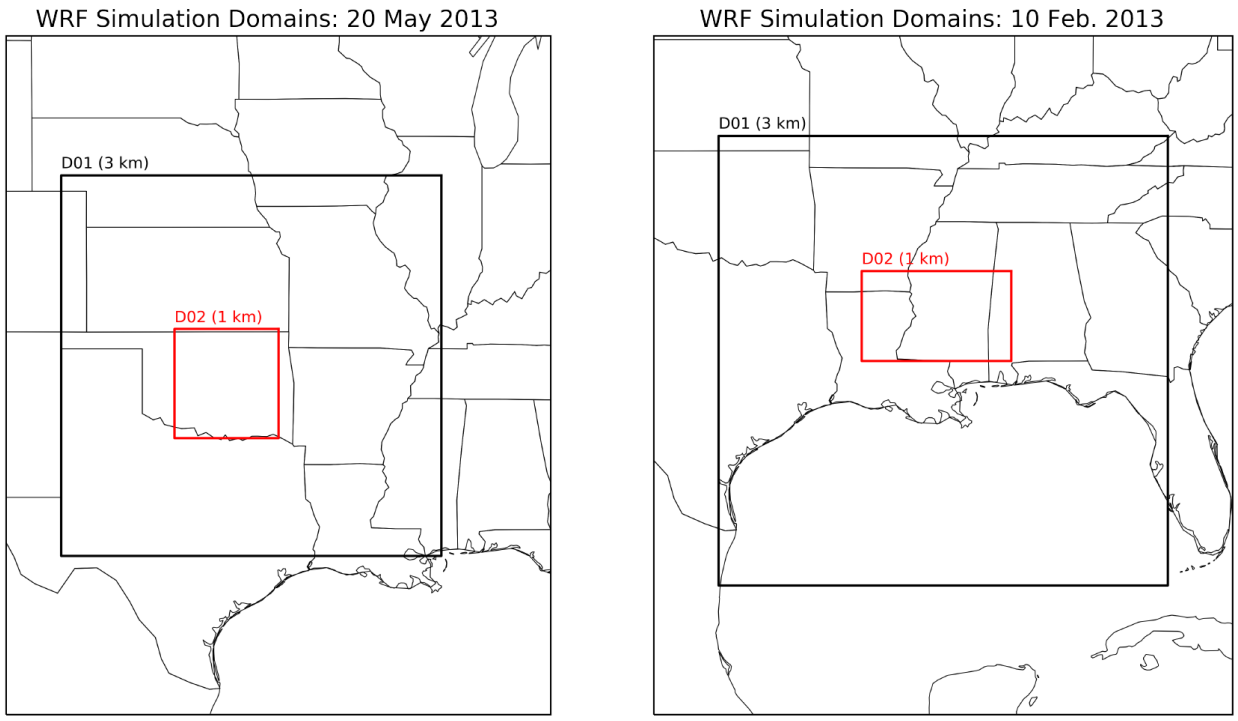

Supplemental Figure S1. Computational domains used for the regional model (WRF) simulations of the 20 May 2013 (WARM) and 10 February 2013 (COOL) events.

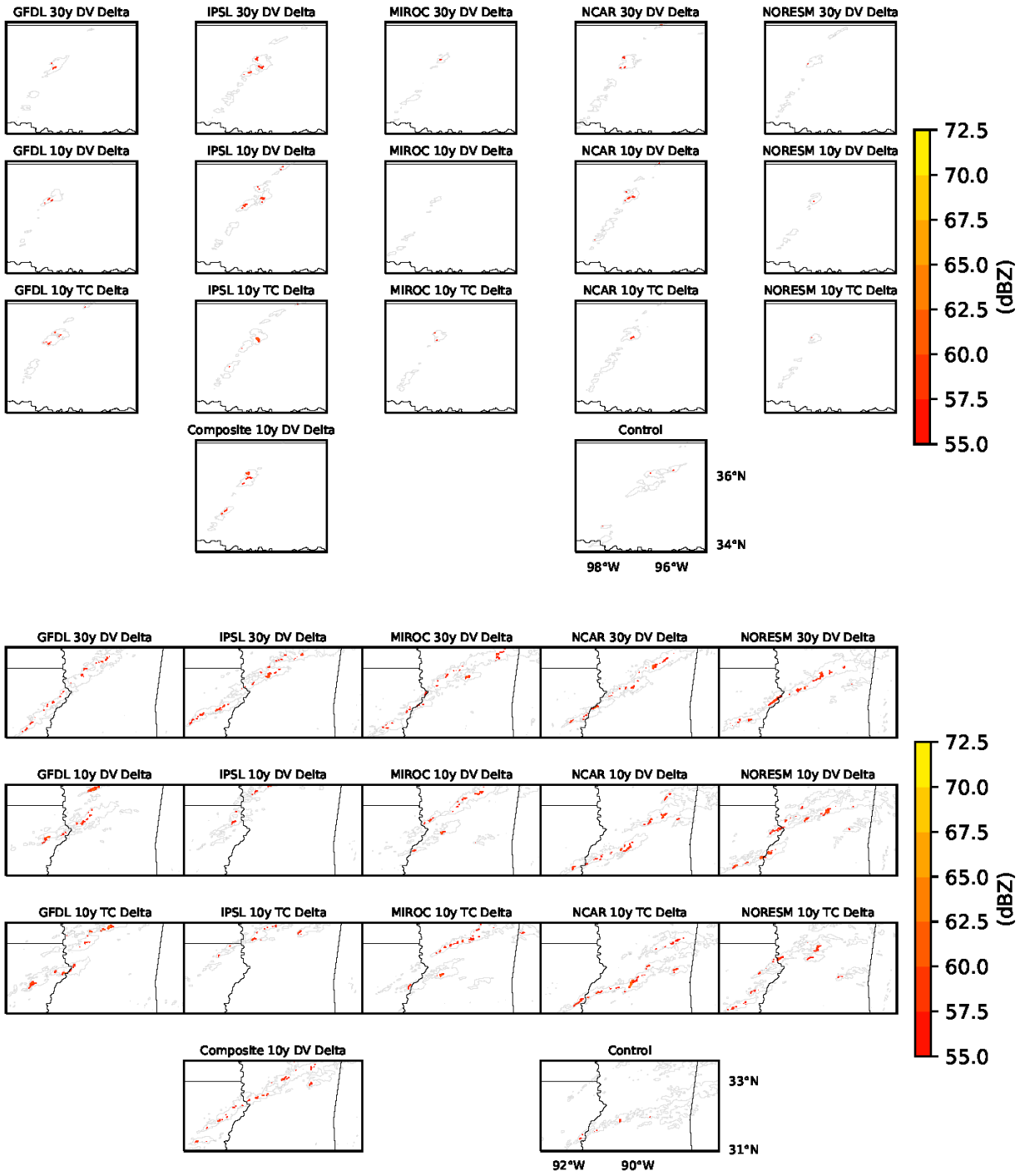

Supplemental Figure S2. Simulated radar reflectivity (dBZ) for the regional-modeling simulations of the WARM event (top panel; 2100 UTC) and COOL event (bottom panel; 0000 UTC). The color fill indicates the areas of intense convective storms over a given simulation. The gray contours are of 30 dBZ radar reflectivity, and show the outline of the convective storms. Each subpanel represents an individual experiment composing the ensemble. See section 2 for guidance on experiment nomenclature.

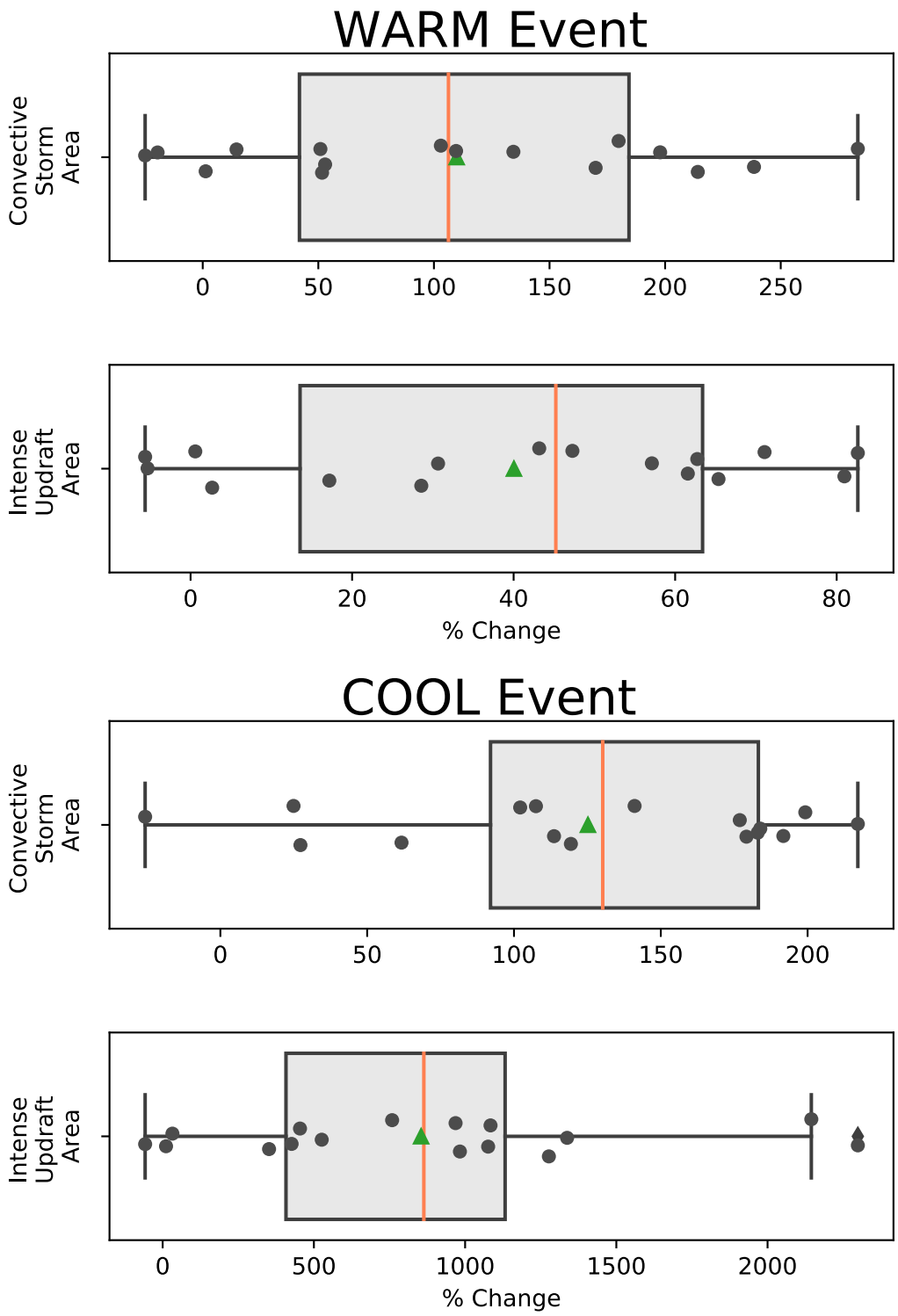

Supplemental Figure S3. Box-and-whisker plots of tornadic-storm intensity-coverage metrics, as evaluated from the regional modeling simulations of the WARM event (top) and COOL event (bottom). Values of these metrics are given as percentage changes in the PGW simulations relative to the control (CTRL) simulation. The median is the orange line, mean is the green triangle, and individual data points are the black circles.

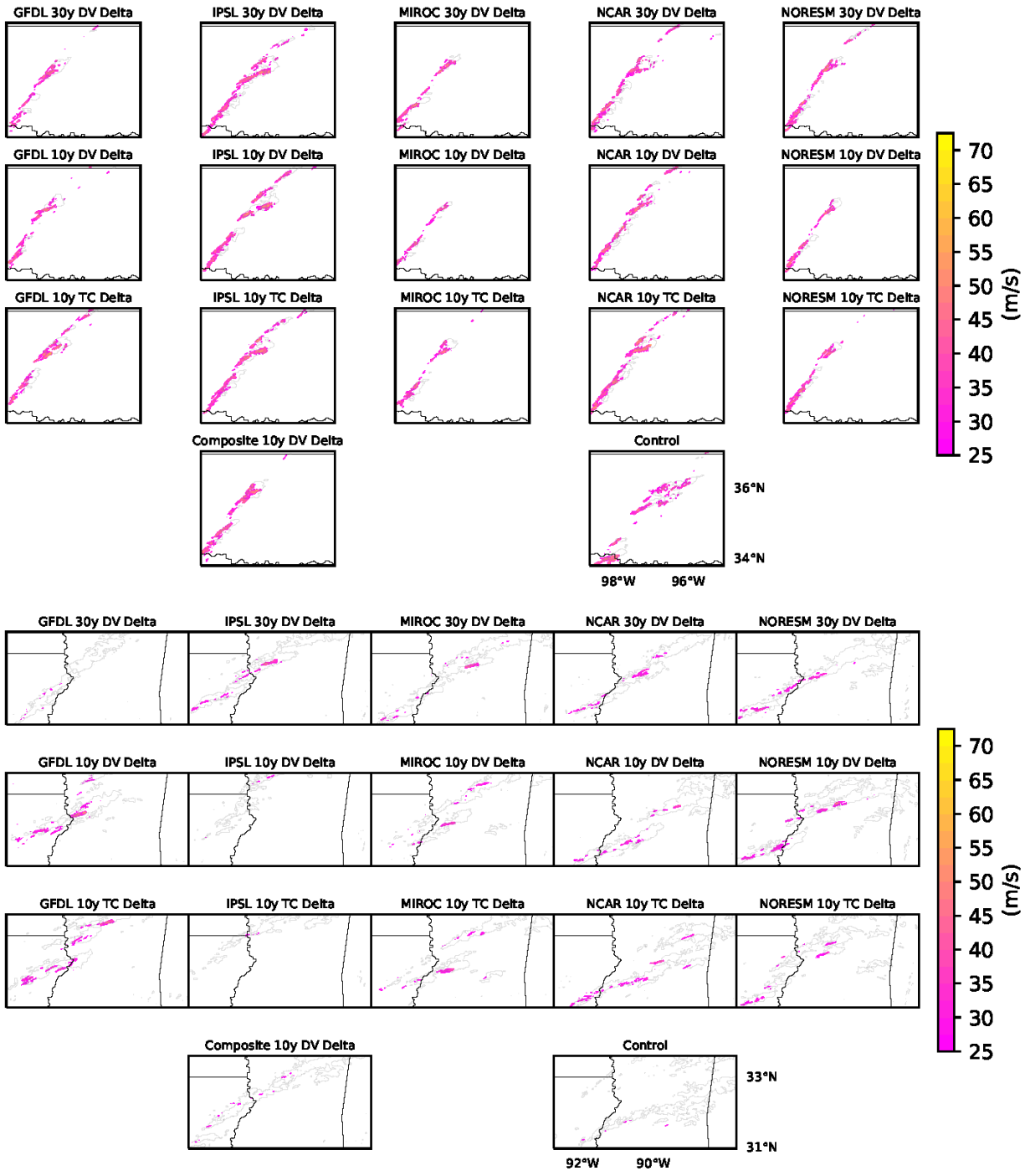

Supplemental Figure S4. Maximum vertical velocity (m/s) for the regional-modeling simulations of the WARM event (top panel; 2100 UTC) and COOL event (bottom panel; 0000 UTC). The color fill indicates the areas of intense updrafts over a given simulation. The gray contours are of 30 dBZ radar reflectivity, and show the outline of the convective storms. Each subpanel represents an individual experiment composing the ensemble. See section 2 for guidance on experiment nomenclature.

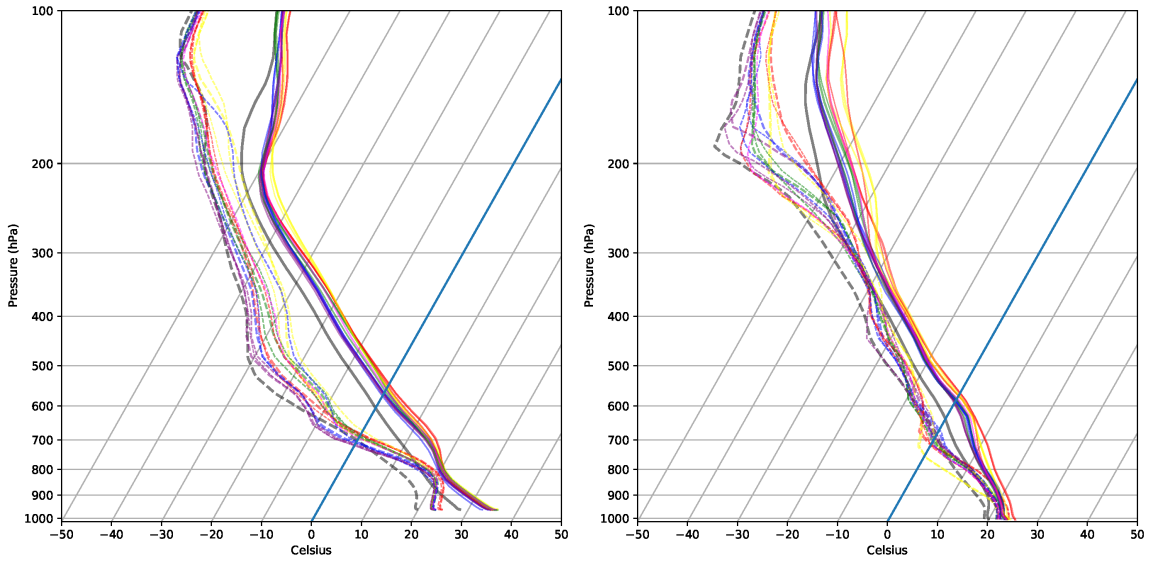

Supplemental Figure S5. Initial and boundary conditions of temperature and dewpoint (°C) for the idealized modeling simulations, for the WARM event (left panel) and COOL event (right panel), as presented on skew-T/log-p diagrams. The solid and dashed black (colored) lines are the temperature and dewpoint for the CTRL (PGW) simulations.

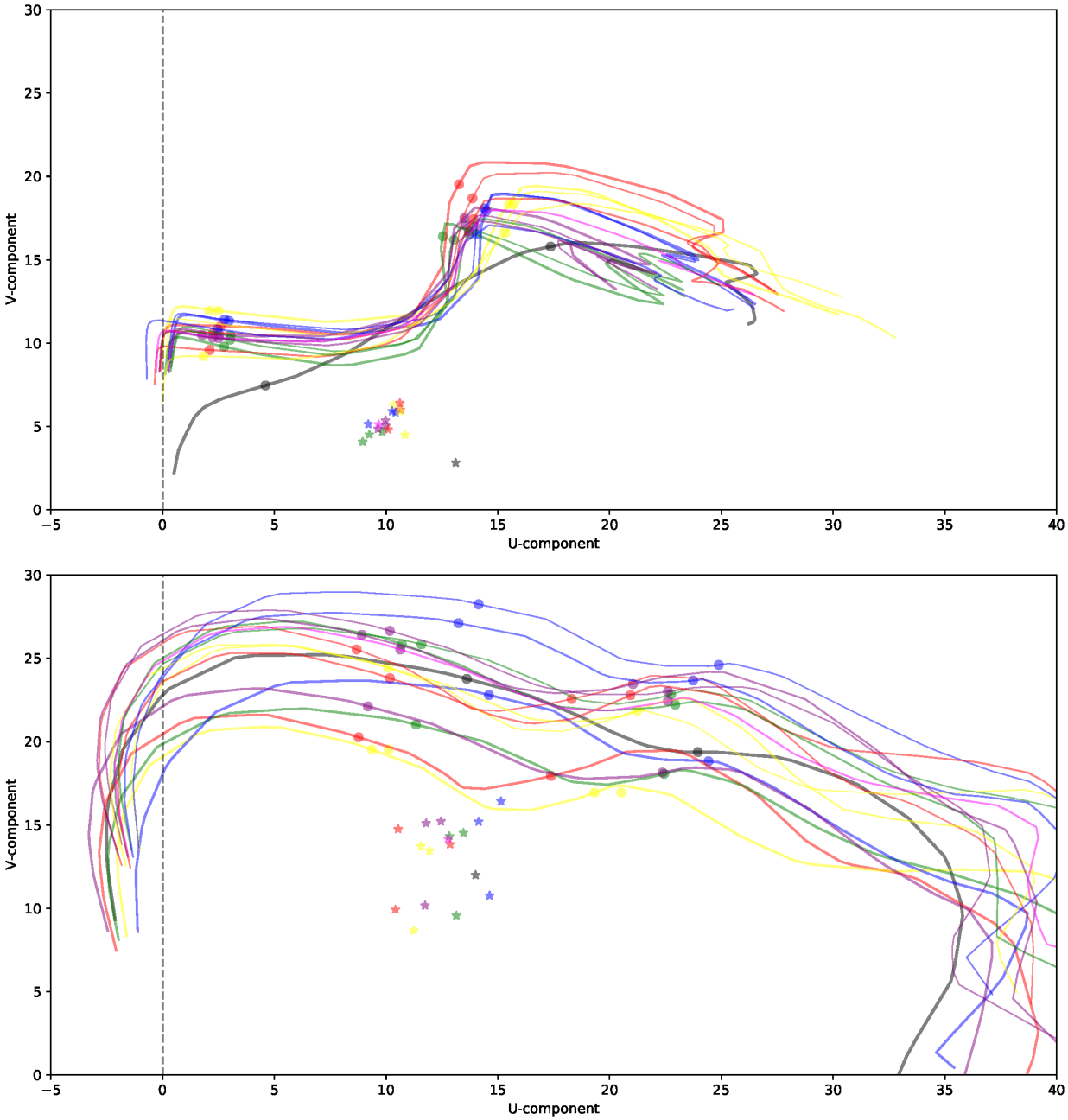

Supplemental Figure S6. Initial and boundary conditions of horizontal wind components (m/s), for the WARM event (top panel) and COOL event (bottom panel), as presented on hodograph plots. The solid (colored) lines are for the CTRL (PGW) simulations. Asterisks show estimated storm motion for a right-moving supercell, and closed circles indicate heights of 1 and 3 km.

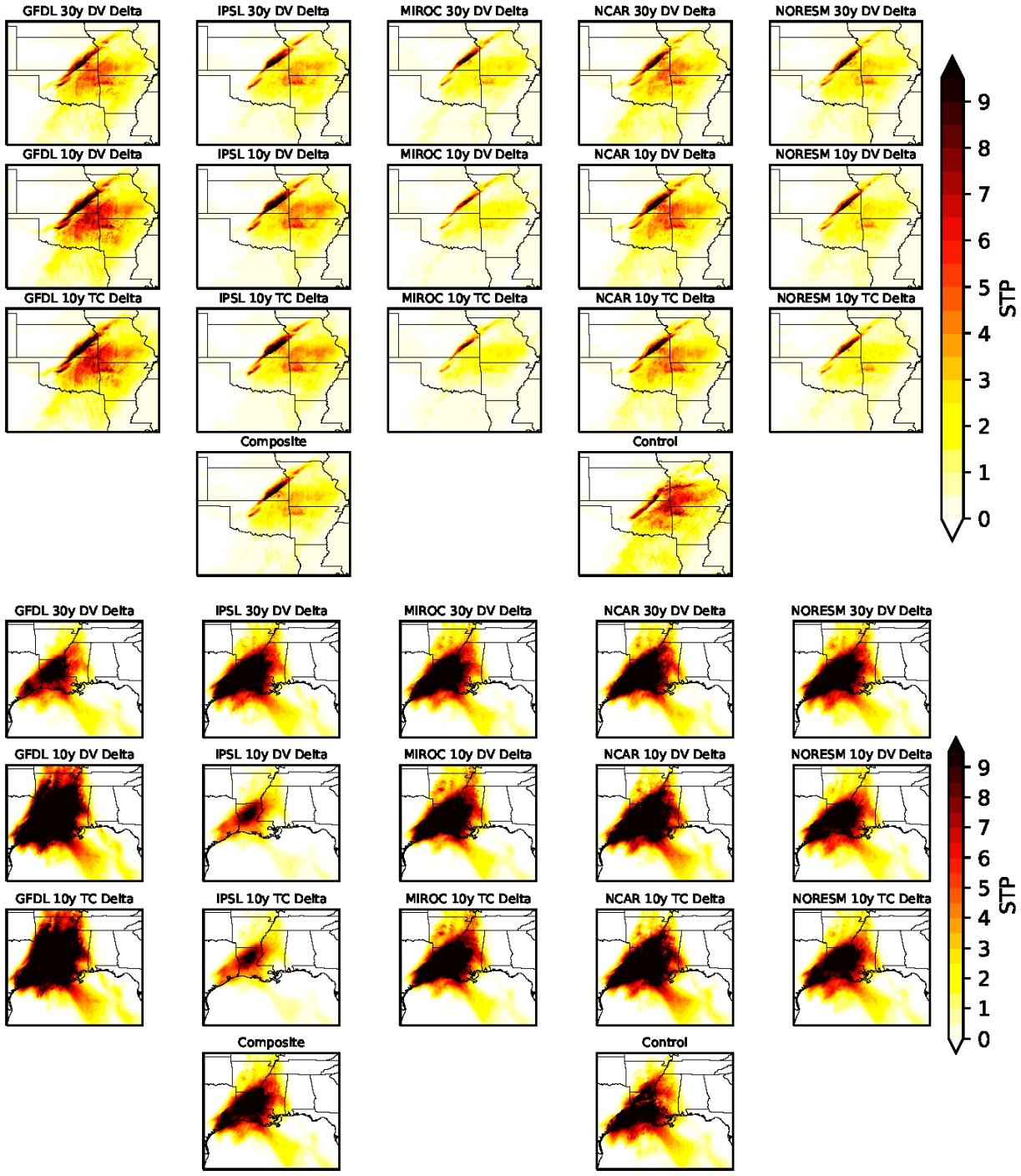

Supplemental Figure S7. Analysis of the significant tornado parameter (STP; nondimensional) over the respective simulation domains (D01; see Fig. S1) of the WARM event (top panel) and COOL event (bottom panel). The calculations were performed using model output at 1800 UTC for the WARM event, and 1500 UTC for the COOL event, which generally represent pre-convective times across the respective simulation domains. See section 2 for guidance on experiment nomenclature.